

1 February 1982

FERMILAB-Proposal-0710

Spokespersons: Jay Orear  
607-256-2328  
Roy Rubinstein  
312-840-4108

MEASUREMENTS OF ELASTIC SCATTERING AND TOTAL CROSS SECTIONS  
AT THE FERMILAB  $\bar{p}p$  COLLIDER

G. Giacomelli, F. Rimondi and Junior Faculty  
University of Bologna, Bologna, Italy

J. Orear and Research Associates and Graduate Students  
Cornell University, Ithaca, New York

W.F. Baker, D.P. Eartly, A.J. Lennox, S.M. Pruss, R. Rubinstein  
and Research Associates  
Fermilab, Batavia, Illinois

M.M. Block, D. Miller and Junior Faculty, Research Associates  
and Graduate Students  
Northwestern University, Evanston, Illinois

MEASUREMENTS OF ELASTIC SCATTERING AND TOTAL CROSS SECTIONS  
AT THE FERMILAB  $\bar{p}p$  COLLIDER

Summary

1. We propose to measure  $\bar{p}p$  total cross sections, the real parts of forward scattering amplitudes, and forward diffraction elastic scattering over the energy range  $\sqrt{s} = 300$  to 2000 GeV.
2. We will normalize our data to the known coulomb scattering cross section. An alternative method of normalization requires a  $4\pi$  detector to record all interactions, both elastic and inelastic, in combination with the small angle detectors. We will either build a  $4\pi$  detector using scintillation counters, or use equivalent signals provided by any other group approved to build a  $4\pi$  detector at D0.

Our apparatus can be used to provide absolute calibration of luminosity monitors for use by other groups.

3. The equipment covers the  $|t|$  range from the coulomb region to  $0.11(\text{GeV}/c)^2$  at  $\sqrt{s} = 300$  and to  $4.8(\text{GeV}/c)^2$  at  $\sqrt{s} = 2000$ . The experiment can be carried out with luminosities of  $\sim 10^{26} \text{cm}^{-2} \text{sec}^{-1}$  or greater. The requested running time is 1300 hours.
4. Locations other than D0 are possible for this experiment, including B0. However, D0 (or A0) has accelerator properties allowing smaller values of  $|t|$  to be reached (see Section VII).
5. In order to measure into the coulomb region, we propose to place detectors in the accelerator lattice by the D14 and C43 quadrupoles. This will require  $\sim 1'$  of room temperature beam pipe at these locations.
6. The detectors in this experiment are small and the apparatus fits into the existing main ring tunnel. We do not require any experimental area to be developed around the intersection region.

MEASUREMENTS OF ELASTIC SCATTERING AND  
TOTAL CROSS SECTIONS AT THE FERMILAB  $\bar{P}P$  COLLIDER

- I. Introduction
- II. Motivation
- III. Experimental Method
- IV. Experimental Equipment
- V. Resolution
- VI. Counting Rates and Estimated Errors
- VII. Location of Experiment
- VIII. Running Conditions
- Appendix A. Some Properties of the Colliding Beams (i)
- Appendix B. Some Properties of the Colliding Beams (ii)

MEASUREMENTS OF ELASTIC SCATTERING AND TOTAL CROSS SECTIONS  
AT THE FERMILAB  $\bar{p}p$  COLLIDER

I. Introduction

We propose to measure  $\bar{p}p$  elastic scattering and total interaction rates at the Fermilab collider up to  $\sqrt{s}$  of 2000 GeV. The  $t$  (four-momentum-squared) range covered will be from the coulomb region ( $|t| < 0.001 \text{ GeV}^2$ ) up to  $|t| \sim 5 (\text{GeV}/c)^2$ . This will enable us to determine:

- (i)  $\sigma_T$ , the total  $\bar{p}p$  cross section,
- (ii)  $\rho$ , the ratio of the real to imaginary part of the forward nuclear scattering amplitude,
- (iii)  $b$ , the slope of the forward diffraction peak,
- (iv) the position of the first diffraction minimum in the elastic scattering,
- (v) the shape and height of the second maximum,
- (vi) the position of the second diffraction minimum (if there is one), or at least the slope beyond the second maximum,
- (vii) The absolute value of the luminosity in our interaction region. This permits calibration of luminosity monitors for all other users at D0.

Data will be taken at several energies between injection ( $\sqrt{s} = 300 \text{ GeV}$ ) and full energy ( $\sqrt{s} = 2000 \text{ GeV}$ ). Both the scattered  $\bar{p}$  and  $p$  will be detected in coincidence using scintillation counters brought close to the circulating beams by means of "Roman Pots" (re-entrant vessels inserted into the accelerator vacuum system). The cross sections are normalized by two independent means: (1) comparison with the known coulomb cross section, and (2) simultaneous measurement of the total interaction rate and small angle elastic scattering. The total interaction rate can be determined using a simple  $4\pi$  scintillation counter array or by using another group's  $4\pi$  scin-

tillation detector signals if available to us.

This experiment does not require any experimental area to be developed at D0: the apparatus required fits into the existing tunnel.

## II. Motivation

### 1. Total Cross Section

The hadron-hadron total cross section  $\sigma_T$  is one of the fundamental measurements needed in any study of hadron interactions. Around 1970, it was believed that all hadron total cross sections had almost reached their expected energy-independent asymptotic values<sup>(1,2)</sup>. A very different picture has emerged from a series of experiments in the 1970's<sup>(3,4,5)</sup>. As energy is increased, all cross sections fall, reach a minimum, and then rise again at high  $s$ . This behavior still does not have a unique explanation. The rising cross sections need to be measured over a large range of  $s$ , in order to establish the functional form of the cross section variation with  $s$ . The cross sections are expected by some to vary only logarithmically with  $s$ . Measurements now extend to the ISR limit of  $\sqrt{s} = 63$  GeV for  $pp$ <sup>(6)</sup> and in preliminary measurements for  $\bar{p}p$  at  $\sqrt{s} = 53$  GeV<sup>(7,8)</sup>; measurements should soon become available from the SPS collider at  $\sqrt{s} = 540$  GeV for  $\bar{p}p$ .

Figure 1 shows some existing data<sup>(1,2,4,5,6)</sup> on  $pp$  and  $\bar{p}p$  total cross sections, together with extrapolations<sup>(9)</sup> to higher energies. At Fermilab Collider energies, the extrapolations are unreliable, and it becomes critical to measure  $\sigma_T$  directly at an  $s$ -value which is a factor of 14 higher than the CERN SPS Collider can achieve.

## 2. The $\rho$ Value

There is an intimate connection between  $\rho$  and the total cross section  $\sigma_T$ . At high energies, the dispersion relation between  $\rho$  and  $\sigma_T$  becomes quasi-local, with  $\rho$  becoming proportional to the logarithmic derivative of  $\sigma_T$ .

Shown in Fig. 2 is the experimental behavior<sup>(9,10)</sup> of  $\rho$  for both  $\bar{p}p$  and  $pp$ , along with dispersion-theory predictions. Starting at very low energies, we see that  $\rho$  decreases with increasing energy, reaches a minimum, goes back through zero, and continues to increase up to ISR energies. Will  $\rho$  continue to increase, or will it reach a maximum and eventually decrease toward zero as expected?<sup>(11)</sup>

We intend to determine  $\rho$  through measurement of the coulomb-nuclear interference term in elastic scattering.

## 3. The Nuclear Slope Parameter

Although the nuclear amplitude for small  $|t|$  ( $\leq 0.02$  (GeV/c)<sup>2</sup>) is adequately parameterized by  $\exp(-b|t|)$ , where  $b$  is a function of  $s$  only, it is known that for larger  $t$ ,  $b$  is a function of both  $s$  and  $t$ <sup>(12)</sup>. This is shown in Figs. 3 and 4. We wish to measure this dependence for large energy and for  $|t|$  in the range 0.001 to 1 (GeV/c)<sup>2</sup>. For small  $t$ , the extrapolation shown in Fig. 3b suggests that  $b$  increases from  $\sim 16$  (GeV/c)<sup>-2</sup> at ISR energies to  $\sim 18$  (GeV/c)<sup>-2</sup> at  $\sqrt{s} = 2000$  GeV. A measurement of this diffractive shrinkage will shed light on the asymptotic behavior of the scattering amplitude.

## 4. First Diffraction Minimum

In 1980 a diffraction dip was first observed at 50 GeV/c at the SPS in  $\bar{p}p$  elastic scattering<sup>(13)</sup> at  $|t| = 1.4$  (GeV/c)<sup>2</sup>, and

subsequently verified at Fermilab at 100 GeV/c<sup>(14)</sup>, as shown in Fig. 5. Some explanations have been given for this behavior, together with predictions for dip position and depth as a function of incident momentum. (15,16)

Using a simple black disc model,  $t_{\text{dip}} \cdot \sigma_T = \text{constant}$ ; assuming  $\sigma_T = 75 \text{ mb}$  at  $\sqrt{s} = 2000 \text{ GeV}$  leads to  $|t|_{\text{dip}} \approx 0.8 \text{ (GeV/c)}^2$ . In Section VI we show that a luminosity of  $10^{28} \text{ cm}^{-2} \text{ sec}^{-1}$  is sufficient to explore details of this first diffraction minimum.

### 5. Second Maximum and Beyond

In pp elastic scattering at beam momenta  $\sim 100 \text{ GeV/c}$  there is only a shoulder in the t distribution at  $|t| \approx 1.4 \text{ (GeV/c)}^2$ ; at ISR energies ( $\sim 1000 \text{ GeV/c}$ ) this grows to a dip and a second maximum an order of magnitude higher than the dip. At even higher ISR energies ( $\sim 1600 \text{ GeV/c}$ ) the dip begins to fill in again. Will the dip in  $\bar{p}p$  disappear at our equivalent beam momentum of  $2 \times 10^6 \text{ GeV/c}$ ? Several theorists have predicted that a second diffraction dip should appear at these energies near  $-t \sim 2.5 \text{ (GeV/c)}^2$ . If no second dip occurs, will the slope after the second maximum remain at the value  $b \approx 2 \text{ (GeV/c)}^{-2}$  observed at lower momenta?

### III. Experimental Method

We plan to measure the elastic scattering rate  $\frac{dN}{dt}$  in the angular region  $0.05 < \theta < 4 \text{ mrad}$  using two sets of small angle scintillation counter hodoscopes. The total interaction rate  $N_T$  will be measured by a  $4\pi$  detector. We will determine  $\sigma_T$ ,  $\rho$  and  $b$  from a simultaneous fit of the measured quantities  $\frac{dN}{dt}$  versus  $t$ , and  $N_T$ .

For elastic  $\bar{p}p$  scattering, the cross-section  $\frac{d\sigma}{dt}$  can be parameterized as:

$$\frac{d\sigma}{dt} = \pi |f_c + f_n|^2. \quad (1a)$$

where  $f_c = 2\alpha \frac{G(t)}{|t|} \exp(-i\alpha\phi(t))$  {coulomb amplitude} (1b)

$f_n = \frac{(1+\rho)}{(4\pi)} \sigma_T \exp(-b|t|/2)$  {nuclear amplitude} (1c)

with  $\alpha$  = fine structure constant

$G$  = proton electromagnetic form factor

Here  $\phi(t)$  is the Yennie-West phase factor for the coulomb amplitude. The optical theorem has been used in (1c), and it has been assumed that  $\rho(t) = \rho(0)$  over the limited  $t$  range covered ( $|t| < 0.02 (\text{GeV}/c)^2$ ).

For measurements made down to sufficiently small values of  $|t|$ , there are 3 distinct scattering regions:

- (i) pure coulomb, (small  $|t|$ )
- (ii) pure nuclear, (large  $|t|$ )
- (iii) coulomb-nuclear interference. (intermediate  $|t|$ )

Measurements in region (ii) allow one to extract  $b$ , whereas region (iii) gives information on  $\rho$ . Region (i) will be used for absolute normalization. At  $\sqrt{s} = 2000$  GeV and assuming  $\sigma_T = 75$  mb (See Fig. 1), the maximum coulomb-nuclear interference occurs at  $|t| = 0.00095 (\text{GeV}/c)^2$ . At  $\sqrt{s} = 300$  GeV, with  $\sigma_T = 55$  mb, the maximum interference is at  $|t| = 0.0013 (\text{GeV}/c)^2$ .

We can write

$$\frac{dN}{dt} = L \frac{d\sigma}{dt} \quad (2)$$

where  $L$  is the luminosity and  $\frac{dN}{dt}$  is the elastic rate corrected for all lost events, e.g., those in which the scattered  $p$  or  $\bar{p}$  is absorbed in the material before the detectors. The value of  $\frac{dN}{dt}$  extrapolated to  $t = 0$ ,  $\left(\frac{dN}{dt}\right)_{t=0}$ , can be expressed, using (1c) as

$$\left(\frac{dN}{dt}\right)_{t=0} = L \frac{(1+\rho^2)}{16\pi} \sigma_T^2 \quad (3)$$

The total counting rate,  $N_T$ , in the  $4\pi$  detector after correction for lost events is given by

$$N_T = L \sigma_T \quad (4)$$

From (3) and (4), one obtains the absolute luminosity

$$L = \frac{N_T^2 (1+\rho^2)}{16\pi \left(\frac{dN}{dt}\right)_{t=0}} \quad (5)$$

and thus the absolute value  $\frac{d\sigma}{dt}$  from (2).

In the low energy region ( $\sqrt{s} \lesssim 1400$  GeV), where we can measure deep into the coulomb region, we can compare the measured values of  $d\sigma/dt$  with the known coulomb cross-section, giving us a method of absolute calibration completely independent of that used in equation (5). The final determinations of  $\sigma_T$ ,  $\rho$ , and  $b$  will be obtained from a best fit to all the input data.

At higher energies ( $\sqrt{s} \gtrsim 1400$  GeV), we cannot reach sufficiently into the pure coulomb region for accurate normalization, and will use only the method of equation (5) to obtain the absolute luminosity; we will still be able to obtain  $\sigma_T$ ,  $\rho$ , and  $b$ .

#### IV. Experimental Equipment

The method proposed to measure elastic scattering is essentially the same as that used in the series of experiments carried out by the CERN-Rome<sup>(4,9,17)</sup> group at the ISR in the early 1970's. The same method is currently being used to measure  $\bar{p}p$  total cross-sections at the ISR<sup>(7)</sup>; a similar technique is used to measure  $\bar{p}p$  total cross-

sections at the SPS collider (UA4).

The method is shown schematically in Fig. 6; the scattering plane is vertical. Each detector consists of small crossed scintillation counter hodoscopes. Two detectors are used at each position as shown, with the results averaged in order to eliminate effects due to uncertainties in knowledge of the beam height.

As noted earlier, there are two sets of detectors (inner and outer) covering different ranges of  $t$ ; their locations are shown schematically in Fig. 7.

The inner detectors, which are located at the ends of the D0 straight section, are 25 meters from the interaction region. Although all details are not final, each detector will consist of  $\sim 20$  vertical counters each  $\sim 2$  mm wide, and  $\sim 25$  horizontal counters, each  $\sim 2$  mm high; a trigger counter covers the entire array ( $\sim 40$  mm x 50 mm). There are four such hodoscope arrays arranged in two pairs, as illustrated in Fig. 6. Assuming that the closest horizontal element can be placed 5 mm from the center of the circulating beams (see Appendix A), the detector covers the polar angular region 0.2 to 2.2 mrad.

The outer detectors are designed to cover smaller polar angles. We take advantage of the Doubler lattice parameters to find a location where the effective distance  $L_{\text{eff}}$  is increased due to the betatron oscillations of the  $p$  and  $\bar{p}$  beams as they circulate around the accelerator.

Let the betatron function and phase at D0 be  $\beta_0$  and  $\psi_0$ , and the corresponding values at a position  $i$  in the lattice be  $\beta_i$ ,  $\psi_i$ . The effective distance  $L_{\text{eff}}$  between D0 and  $i$  can be shown to be

$$L_{\text{eff}} = (\beta_0 \beta_i)^{\frac{1}{2}} \sin (\psi_i - \psi_0) \quad (6)$$

Parameters for the vertical plane are <sup>(18)</sup>  $\beta_0 = 106.16$  m, and  $\psi_0 = 9.546 \times 2\pi$  radians.

For the circulating protons, if we chose  $i$  to be the location of the D14 quadrupole (123 m from the collision region), we find  $\beta_{14} = 97.54$  m and  $\psi_{14} = 9.808 \times 2\pi$  radians. This gives

$$\Delta\psi = (\psi_{14} - \psi_0) = 94.62^\circ, \quad \sin \Delta\psi = 0.997.$$

$$L_{\text{eff}} = 101.5 \text{ meters.}$$

Similarly for antiprotons, a detector at C43 (210 m from the collision region) will have

$$\Delta\psi = 255.6^\circ, \quad \sin \Delta\psi = 0.969$$

$$L_{\text{eff}} = 98.78 \text{ m.}$$

These outer detectors will be hodoscope arrays similar to the inner detectors, each consisting of  $\sim 20$  vertical counters, each  $\sim 2$  mm wide and  $\sim 20$  horizontal counters, each  $\sim 1$  mm high. The trigger counters will be  $\sim 40$  mm wide by 20 mm high. They would also be mounted in "Roman Pots" which we again assume can be moved in as close as 5 mm to the centers of the circulating beams. The range of scattering angles covered would then be 0.05 to 0.25 mr. This

method of making use of the lattice parameters reaches a  $|t|$  value 16 times smaller than having the small angle detectors at the ends of the straight section. Table 1 gives the  $t$  ranges covered by the detectors.

Since measurements over some regions of  $t$  can be made with both the inner and outer detectors, we will have a check on the method of using detectors in the accelerator lattice. As a by-product, a measurement of the accelerator betatron parameters should be obtained.

If low- $\beta$  quadrupoles (giving  $\beta \approx 3$  m?) are available at D0,  $L_{\text{eff}}$  is reduced considerably, and the  $t$  region subtended by the outer detectors becomes comparable to that of the inner detectors under the high- $\beta$  conditions discussed up to now. Since there are  $>100$  m of superconducting Doubler magnets between D0 and the detectors, we will have good magnetic analysis on both outgoing particles to remove inelastic background from these large  $|t|$  measurements.

As in the ISR experiment,<sup>(7)</sup> ADC information will be recorded for all counters, and TDC information will be recorded for the 8 trigger counters. Each hodoscope array will be positioned remotely.

For measuring the total interaction rate, we will use a  $4\pi$  detector composed of scintillation counters surrounding the interaction region. As an illustration of such a detector, Fig. 8 shows the detector used by the Pisa-Stony Brook group at the ISR.<sup>(19)</sup> If another group is approved to carry out an experiment using a  $4\pi$  detector at D0, we could use the signals from their scintillation counters to perform this measurement.

Relative luminosity monitoring will be provided by a set of scintillation counters placed near the ends of the D0 straight section. Our experiment will calibrate these monitors for use by any other experiment there.

### V. Resolution

A finite beam size of standard deviation  $\sigma$  at the interaction point causes a point in detector H1 to correspond to a size  $\sigma_{H2} = 2\sigma$  at detector H2, as shown in Fig. 9. The effect of the angular divergence of the two beams must be added to this in quadrature.

The total standard deviation on array H<sub>2</sub> (corresponding to a point on H1) is

$$\sigma_{H2}^2 = \frac{4 \sigma_p^2 \sigma_{\bar{p}}^2}{\sigma_p^2 + \sigma_{\bar{p}}^2} + L^2 (\theta_p^2 + \theta_{\bar{p}}^2)$$

where  $\sigma_p$ ,  $\sigma_{\bar{p}}$  are the widths of the two beams, and  $\theta_p$ ,  $\theta_{\bar{p}}$  are their r.m.s. divergences. For the outer detectors, using  $\sigma_p = \sigma_{\bar{p}} = 1.8$  mm,  $L_{\text{eff}} = 100$  m,  $\theta_p = \theta_{\bar{p}} = 0.017$  mr (conservative estimates derived in Appendix A), we obtain  $\sigma_{H2} = 3.5$  mm. As discussed in Appendix B, another term in the betatron transfer matrix from D0 to location i gives an additional effect of about the same magnitude. For the inner detector at  $L = 25$  m,  $\sigma_{H2} = 2.6$  mm.

From the size of  $\sigma_{H2}$  (several mm) we conclude that adequate spatial resolution is achieved with hodoscope elements of  $\sim 1$  mm. In particular, there is no advantage in attaining resolutions of  $\sim 100$  microns using silicon detectors or drift chambers for the elastic

scattering measurements. A detailed analysis of the unfolding of beam resolutions, cross section variations across the hodoscope, etc. has been performed analytically for finite size counters. (20) Basically, the distribution of elastic events over the hodoscope elements contains all the information needed to extract beam parameters and differential cross sections for use in equations 1a, 1b and 1c; the ISR results show that this technique works with high precision.

#### VI. Counting Rates and Estimated Errors

Even at very low luminosity, the low  $|t|$  hodoscope elements have high counting rate. We take  $\frac{d\sigma}{dt} = Ae^{-b|t|}$ , with  $b = 18 \text{ (GeV/c)}^{-2}$  and  $A = 2.87 \cdot 10^{-25} \text{ cm}^2 \text{ (GeV/c)}^{-2}$  obtained from the optical theorem with  $\sigma_T = 75 \text{ mb}$  and  $\rho = 0$ . Then in the region  $0.001 < |t| < 0.1 \text{ (GeV/c)}^2$ , we obtain about 300,000 counts per hour in our system at a luminosity of  $10^{28} \text{ cm}^{-2} \text{ sec}^{-1}$ . Clearly  $\sigma_T$ ,  $\rho$ , and  $b$  can easily be determined even if the intensity is down by two orders of magnitude.

In estimating the cross section in the dip region ( $|t| = 0.8 \text{ (GeV/c)}^2$ ) we assume the slope changes from  $b=18$  to  $15 \text{ (GeV/c)}^{-2}$  at  $|t|=0.2 \text{ (GeV/c)}^2$  (this is the same amount of change of slope as observed at the ISR). Then  $\frac{d\sigma}{dt} \sim 10^{-30} \text{ cm}^2 \text{ (GeV/c)}^{-2}$  at the dip. Using a luminosity of  $10^{28} \text{ cm}^{-2} \text{ sec}^{-1}$  and  $\Delta t = 0.1 \text{ (GeV/c)}^2$ , the rate would be 1.6 events/hr. In the region of the second maximum and beyond, we take the pessimistic assumption that  $\frac{d\sigma}{dt}$  does not rise above the dip and that beyond  $|t| = 1.3 \text{ (GeV/c)}^2$  the slope is  $b=2 \text{ (GeV/c)}^{-2}$  (as observed at

the ISR). Then at  $|t| = 3 \text{ (GeV/c)}^2$  with  $\Delta t = 0.5 \text{ (GeV/c)}^2$ , a luminosity of  $10^{28} \text{ cm}^{-2} \text{ sec}^{-1}$  would give 4 events per day.

We conclude that the expected counting rates are adequate at luminosities of  $10^{28} \text{ cm}^{-2} \text{ sec}^{-1}$ . Even for luminosities of  $10^{26} \text{ cm}^{-2} \text{ sec}^{-1}$ , we have adequate counting rates for determining  $\sigma_T$ ,  $b$  and  $\rho$ ; the recent CERN ISR  $\bar{p}p$  experiments<sup>(7,8)</sup> using luminosities  $\sim 10^{26} \text{ cm}^{-2} \text{ sec}^{-1}$  achieved statistical precisions, in several hours of running, of  $\sim 5\%$  in  $\sigma_T$ , and measured elastic scattering out to  $|t|$  of  $0.6 \text{ (GeV/c)}^2$ .

The rates and acceptance of our system may permit measurements to  $|t| \sim 5 \text{ (GeV/c)}^2$ ; however the inelastic background will probably be larger than the signal in the high  $|t|$  region. Similar elastic scattering experiments in which only the angle-angle correlation is measured start having background problems at  $|t| \sim 1.5 \text{ (GeV/c)}^2$ . Even though we can determine the inelastic background with good statistical precision, we can not expect to reach much farther than  $|t| \sim 1.5 \text{ (GeV/c)}^2$  without momentum analysis. If there is to be any low beta running at D0, then as mentioned previously, the Doubler accelerator magnets provide a good momentum resolution for the scattered  $\bar{p}$  and  $p$ .

Based on ISR experience, the inelastic background at small  $|t|$  in the inner detectors may readily be obtained from the pattern of events in the hodoscopes. It is generally small; for example, in the region  $|t| < 0.04 \text{ (GeV/c)}^2$ , it should be less than 0.5%.<sup>(7)</sup> Background in the outer detectors should be much less because of the considerable magnetic analysis provided by the Doubler accelerator magnets.

Again from experience at the ISR, systematic uncertainties in the value of  $\sigma_T$  should be  $\sim 0.5\%$  (4,6,17). For  $\rho$ , systematic uncertainties should be  $\sim 0.01$ . (9)

### VII. Location of Experiment

We propose this experiment for the D0 straight section, although there are other possible locations that are less desirable. The major requirement is to have a high  $\beta$  at the intersection region in order to have the beams as parallel as possible.

At both A0 and D0,  $\beta = 106$  m; the other 4 straight sections (B0, C0, E0, F0) all have  $\beta = 73$  m. (18) If we use 5 mm as an estimate of how close a detector can be placed to the circulating beam, and then find a location in the lattice where  $\sin \Delta\psi \sim 1$  and  $\beta \sim 100$  m, the minimum values of  $|t|$  at  $\sqrt{s} = 2000$  GeV are:

A0, D0	$2.4 \cdot 10^{-3} \text{ (GeV/c)}^2$
B0, C0, E0, F0	$3.4 \cdot 10^{-3} \text{ (GeV/c)}^2$

Thus it is possible to carry out this experiment at B0, but data will not be obtained as far into the coulomb region as at D0. In addition, we expect B0 to be occupied by the Collider Detector Facility; this facility will need low  $\beta$  ( $\sim 3$  m) quadrupoles on for high luminosity most of the time, which precludes small  $t$  measurements.

### VIII. Running Conditions

We need to turn off the low  $\beta$  quadrupoles at D0 in order to have the two crossing beams as parallel as possible during the low  $|t|$  running. As discussed earlier, low  $\beta$  quadrupoles will enable us to make measurements in the range  $|t| \gtrsim 1.5 \text{ (GeV/c)}^2$ .

The detectors require about 1 foot of beam pipe, at the ends of the D0 straight section, to install the "Roman Pots" containing the detectors. In addition, we will need about 1 foot of room temperature beam pipe at the D14 and C43 locations for the other set of detectors. This latter requirement is not trivial since, as currently designed, the beam pipes there are at liquid helium temperatures. However, conversations with many members in the Accelerator Division have indicated that such a change is possible, although needing detailed engineering design.

We wish to run this experiment at several energies between  $\sqrt{s} = 300$  and 2000 GeV. Measurements overlapping with the SPS Collider will be valuable to understand systematic effects; the lower energy data, which will enable us to reach lower values of  $|t|$ , will allow a study further into the coulomb region, which is needed for equipment calibration.

The running time needed for the experiment depends on the luminosity and the number of different energies studied; 200 hours at each energy should allow measurements to  $|t| \approx 0.8 (\text{GeV}/c)^2$  even with  $10^{26} \text{ cm}^{-2} \text{ sec}^{-1}$  luminosity. Measurements at 5 energies, with 300 hours for testing, lead to a total request of 1300 hours.

We note that this experiment does not require any experimental area to be developed at D0; our experiment fits into the existing tunnel, and only a counting area nearby is needed.

TABLE 1 - Values of the Minimum and Maximum Values of  $|t|$  at  
Different Values of  $\sqrt{s}$ .

$\sqrt{s}$ (GeV)	<u>Inner Detector</u>		<u>Outer Detector</u>		mr (GeV/c) <sup>2</sup>
	$\theta_{\min}=0.2$ $ t _{\min}$	$\theta_{\max}=2.1$ $ t _{\max}$	$\theta_{\min}=0.05$ $ t _{\min}$	$\theta_{\max}=0.25$ $ t _{\max}$	
300	0.0009	0.11	0.000056	.0014	
500	0.0025	0.30	0.00016	.0039	
1000	0.01	1.2	0.00063	.016	
1500	0.023	2.7	0.0014	.035	
2000	0.04	4.8	0.0025	.063	

## References

1. K.J. Foley et al. Phys. Rev. Lett. 19, 857 (1967)
2. W. Galbraith et al. Phys. Rev. 138, B913 (1965)
3. S.P. Denisov et al. Phys. Lett. 36B, 415 (1971)
4. U. Amaldi et al. Phys. Lett. 44B, 112 (1973)
5. A.S. Carroll et al. Phys. Lett. 61B, 303 (1976) and 80B, 423 (1979)
6. CERN-Pisa-Rome-Stony Brook, Phys. Lett. 62B, 460 (1976)
7. D. Favart et al. Phys. Rev. Lett. 47, 1191 (1981) and M. Block - private communication
8. G. Carboni et al. CERN preprint, CERN-EP/81-141 (1981)
9. U. Amaldi, et al. Phys. Lett. 66B, 390 (1977)
10. L.A. Fajardo et al. Phys. Rev. D24, 46 (1981)
11. R.E. Hendrick and B. Lautrup. Phys. Rev. D11, 529 (1975)
12. A. Schiz et al. Phys. Rev. D24, 26 (1981)
13. Z. Asa'd et al. CERN preprint, CERN-EP/81-26 (1981)
14. Roy Rubinstein, Fermilab Report, October 1981, p.1, and W.F. Baker et al., to be published.
15. M.M. Islam and J.P. Guillard, University of Connecticut preprint (1981)
16. T.T. Chou and C.N. Yang, Phys. Rev. Lett. 46, 764 (1981)
17. U. Amaldi et al. Phys. Lett. 43B, 231 (1973)
18. Superconducting Accelerator Design Report, Fermilab 1979, Appendix II, p.A4
19. S.R. Amendolia et al. Phys. Lett. 44B, 119 (1973). See also ref. 6.
20. N. Amos, M.M. Block, C. Leroy, S. Zuchelli, ISR R211 experiment note. See also ref. 7.

21. Superconducting Accelerator Design Report, Fermilab 1979, Appendix 1, p.A1.
22. Ibid, p.174.
23. Ibid, p.196.
24. Tevatron Phase I Design Report, Fermilab 1980, p.29.

## FIGURE CAPTIONS

- Fig. 1     $pp$  and  $\bar{p}p$  total cross sections versus  $\sqrt{s}$ . An extrapolation of the data to collider energies is also indicated.
- Fig. 2    The ratio  $\rho$  of the real to the imaginary part of the forward scattering amplitudes for  $pp$  and  $\bar{p}p$  elastic scattering plotted versus lab momentum.
- Fig. 3    (a) The  $t$  dependence of the slope parameter  $b$  for  $\pi^-p$ ,  $\pi^+p$  and  $pp$  elastic scattering at 200 GeV/c.  
(b) The energy dependence of the slope parameter  $b$ , computed at an average value of  $|t| = 0.05 \text{ (GeV/c)}^2$  for  $pp$  elastic scattering.
- Fig. 4    The  $pp$  and  $\bar{p}p$  slope parameter  $b$ , computed at different average values of  $|t|$  plotted versus lab momentum.
- Fig. 5    Compilation of data on  $\bar{p}p$  elastic scattering around the first diffraction minimum and the second maximum, from refs. 13 and 14.
- Fig. 6    Schematic experimental layout, side view. The figure shows the "Roman Pots" and the detectors.
- Fig. 7    Accelerator layout (schematic) near D0, showing locations of the detector arrays.
- Fig. 8    Layout of the  $4\pi$  detector used by the Pisa-Stony Brook group (ref. 19).
- Fig. 9    Illustration of the resolution calculation.

## Appendix A. Some Properties of the Colliding Beams (i)

The resolution needed in the detectors is determined by the properties of the two crossing beams at the intersection point.

The expected emittance  $\epsilon$  of the beam is given in a number of references:

$$(i) \quad \epsilon (150 \text{ GeV}) = <0.2\pi \text{ mm.mr} \quad (2\sigma) \quad (\text{Ref 21})$$

$$\therefore \epsilon (1000 \text{ GeV}) = <0.03\pi \text{ mm.mr}$$

$$(ii) \quad \epsilon (150 \text{ GeV}) = 0.15\pi \text{ mm.mr} \quad (95\%) \quad (\text{Ref 22})$$

$$\therefore \epsilon (1000 \text{ GeV}) = 0.02\pi \text{ mm.mr}$$

$$(iii) \quad \text{Beam size} = \pm 1.2 \text{ mm at } \beta=70 \text{ m at } 1000 \text{ GeV} \quad (\text{Ref 23})$$

$$\therefore \epsilon (1000) = \frac{\text{size}^2 \pi}{\beta} = 0.02 \pi \text{ mm.mr}$$

$$(iv) \quad \epsilon (1000) \text{ proton} = 0.026 \pi \text{ mm.mr} \quad (\text{Ref 24})$$

$$\epsilon (1000) \text{ antiproton} = 0.01 \pi \text{ mm.mr.}$$

We will use  $\epsilon(1000) = 0.03 \pi \text{ mm.mr}$  as a conservative estimate of the emittance of each beam. This gives at D0 ( $\beta=106.16 \text{ m}$ ) a vertical beam size

$$\pm \left( \frac{\epsilon \beta}{\pi} \right)^{\frac{1}{2}} \text{ equal to } \pm 1.8 \text{ mm, and a}$$

vertical beam divergence

$$\pm \left( \frac{\epsilon}{\beta \pi} \right)^{\frac{1}{2}} \text{ equal to } \pm 0.017 \text{ mr.}$$

Horizontal sizes are calculated to be somewhat larger because of the finite energy spread of the beams; this is an important reason to measure elastic scattering in the vertical plane. The beam size of  $\pm 1.8 \text{ mm}$  leads us to believe that detectors may be placed as close as  $\sim 5 \text{ mm}$  from the beam center.

Appendix B. Some Properties of the Colliding Beams (ii)

The displacement  $d_i$  from the nominal beam orbit at position  $i$  for a particle starting at position  $o$  with angle  $\theta_o$  and displacement  $d_o$ , is given by

$$d_i = \left( \frac{\beta_i}{\beta_o} \right)^{\frac{1}{2}} \{ \cos(\psi_i - \psi_o) + \alpha_o \sin(\psi_i - \psi_o) \} d_o + (\beta_o \beta_i)^{\frac{1}{2}} \sin(\psi_i - \psi_o) \theta_o$$

where  $\alpha_o$  is another betatron parameter. {Equation (6) in Section IV is the last term of this expression}.

At D0,  $\alpha_o = -1.968$ . For  $i = D14$ , the first term becomes  $-1.96 d_o$ . A spread in  $d_o$  of  $\pm 1.8$  mm then leads to a variation in  $d_i$  of  $\pm 3.5$  mm.

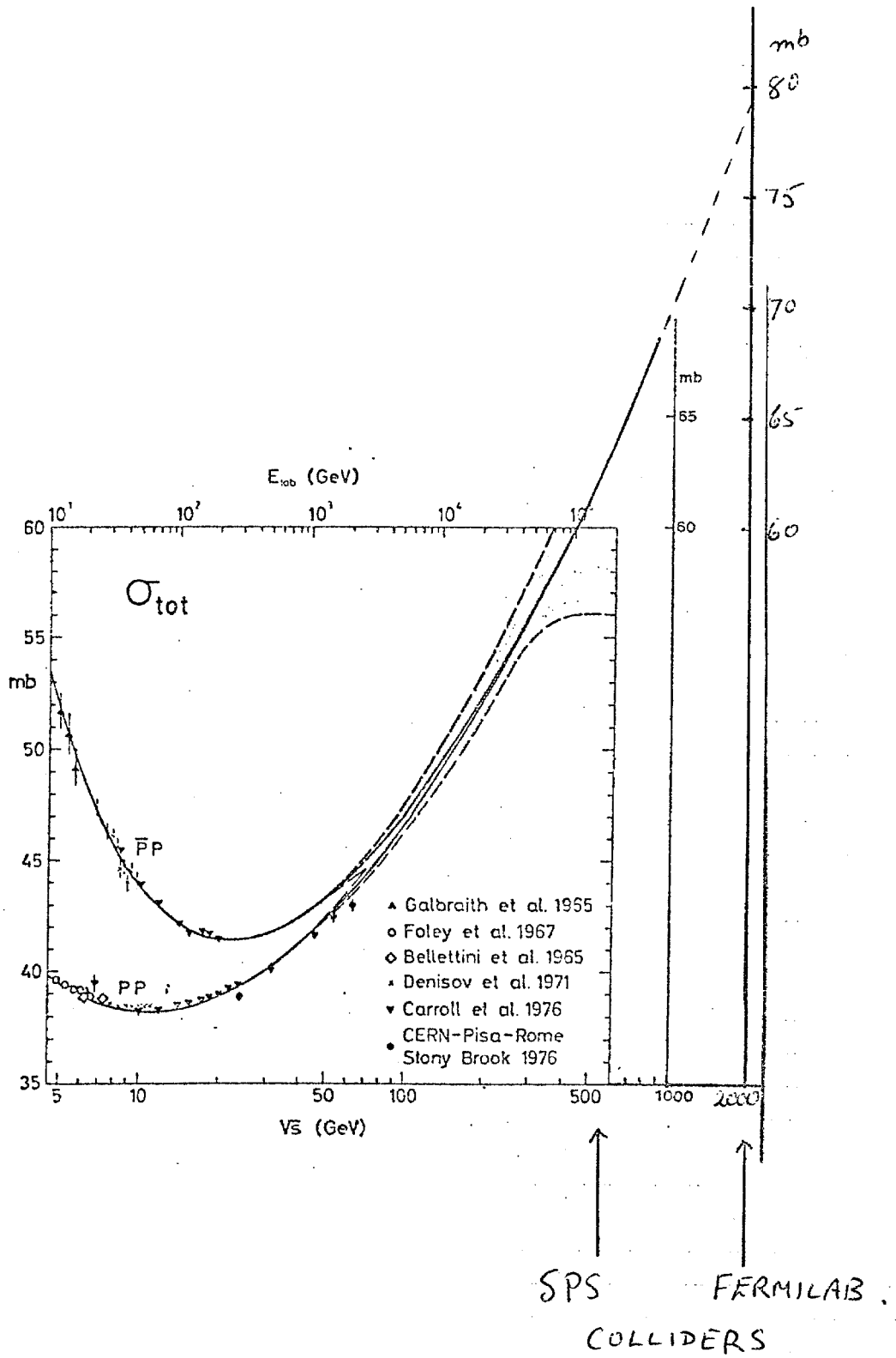


FIG. 1.

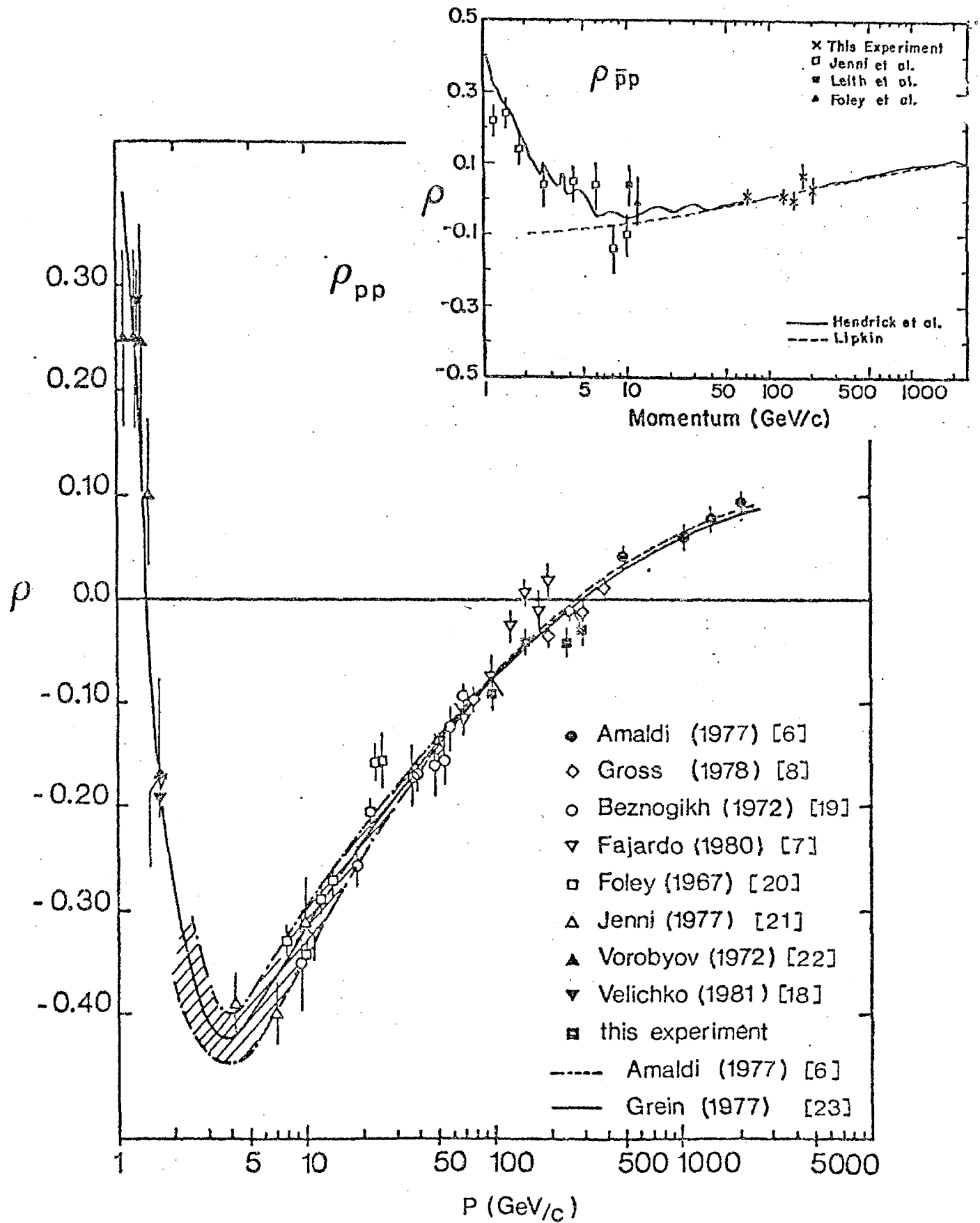
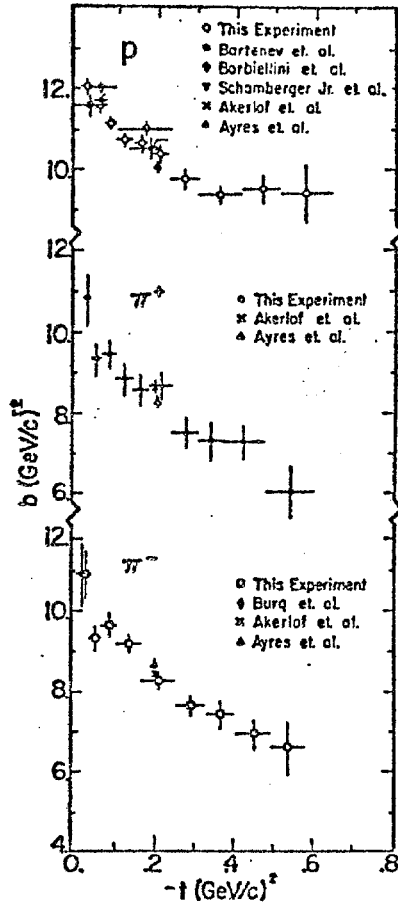


FIG. 2.

a)



b)

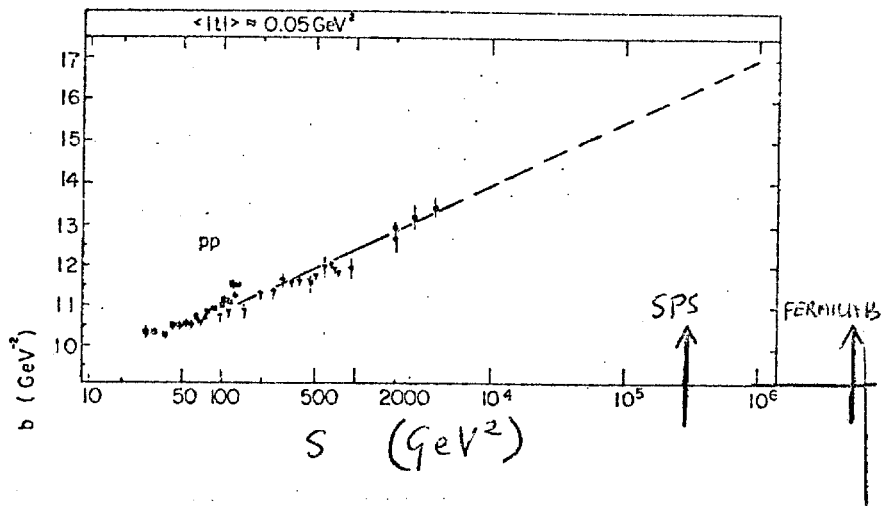


FIG. 3.

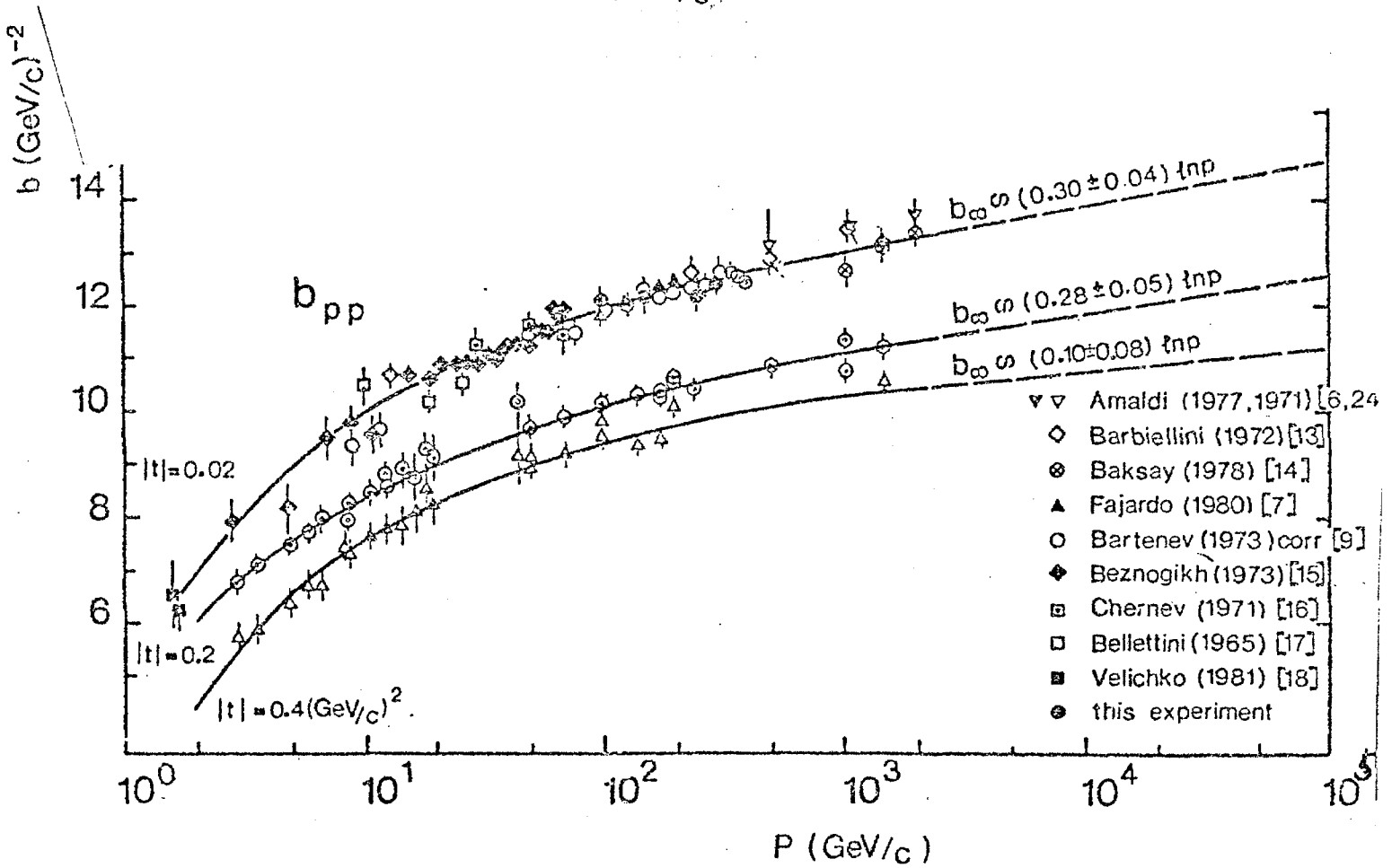
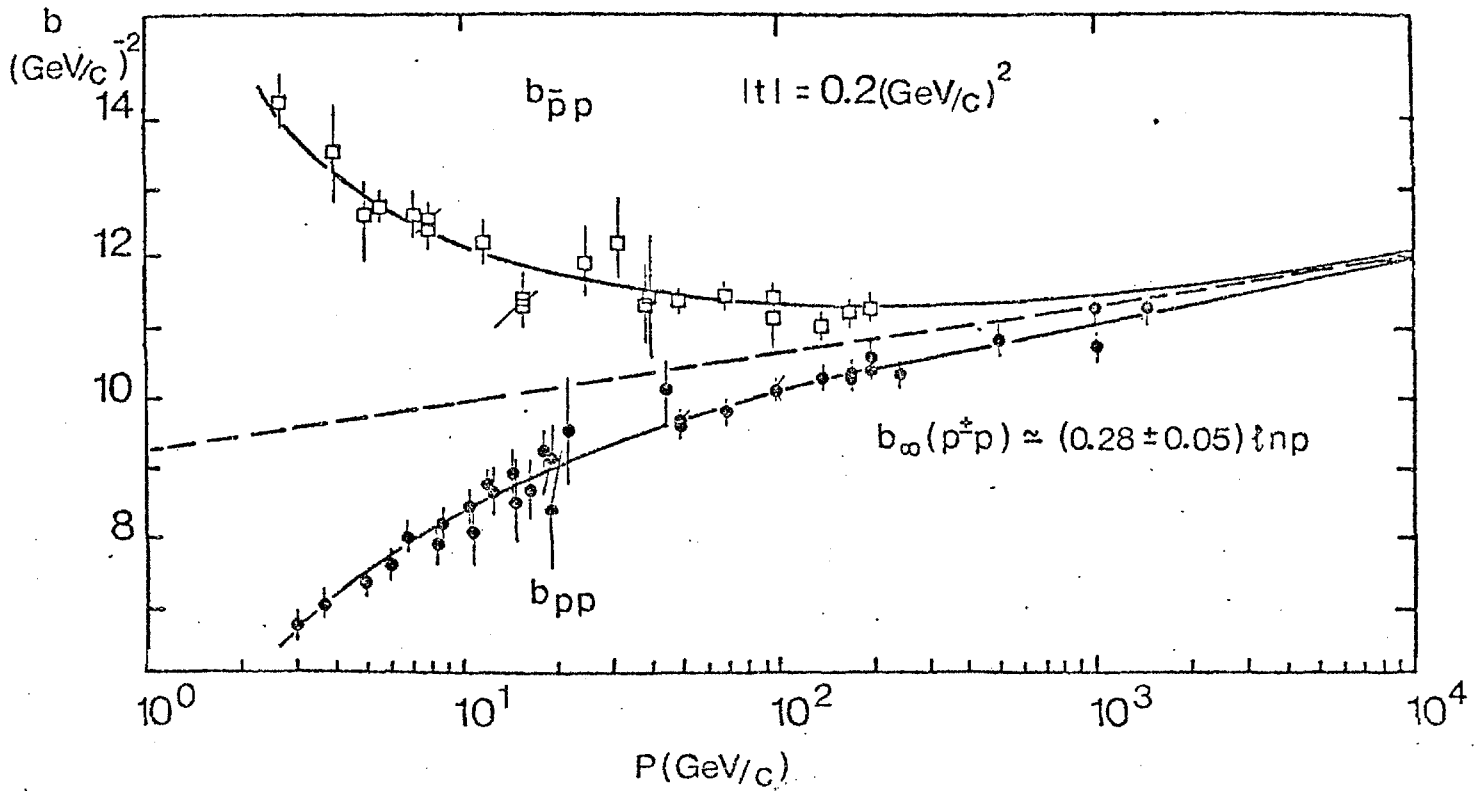


FIG. 4.

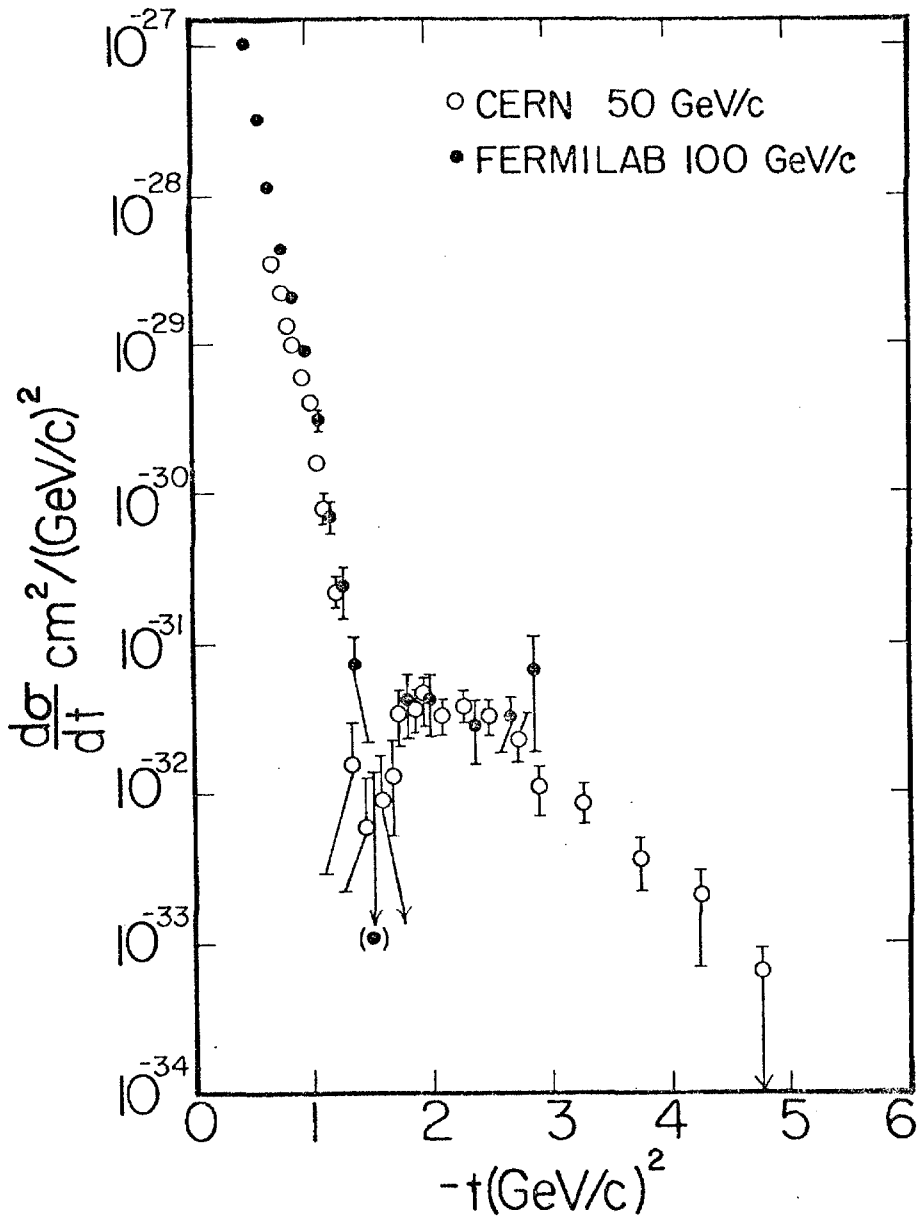


FIG. 5.

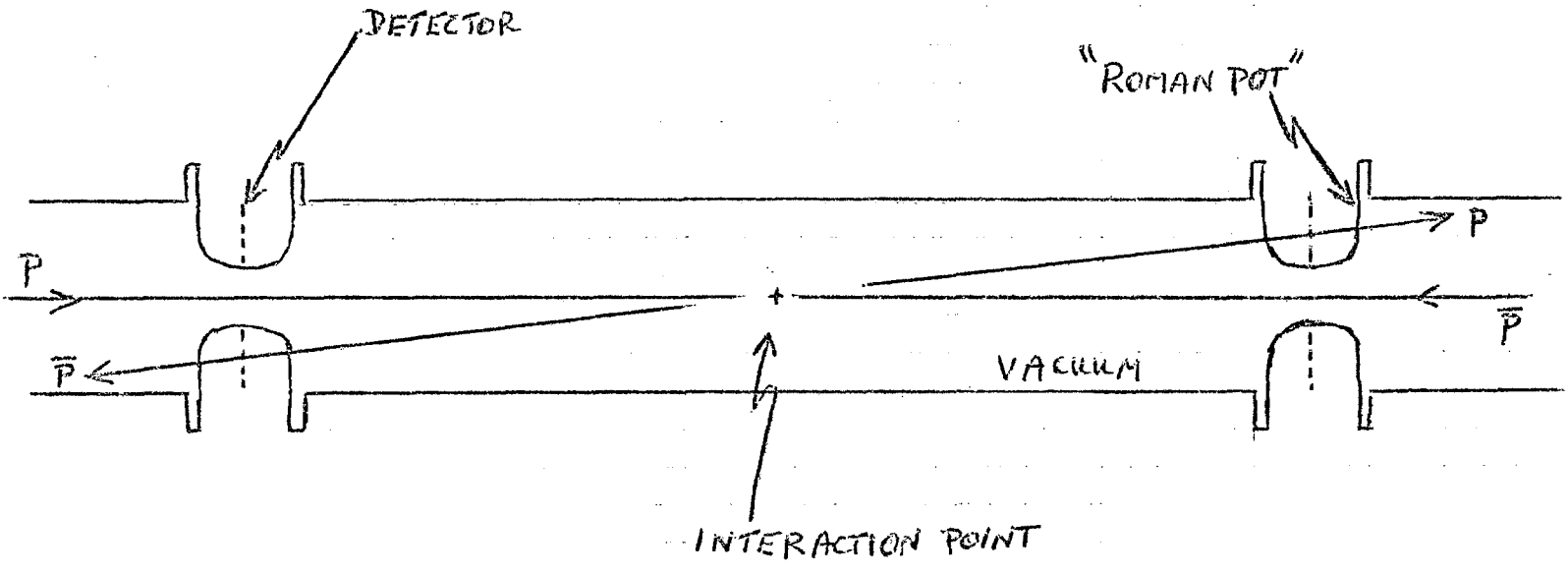


FIG. 6.

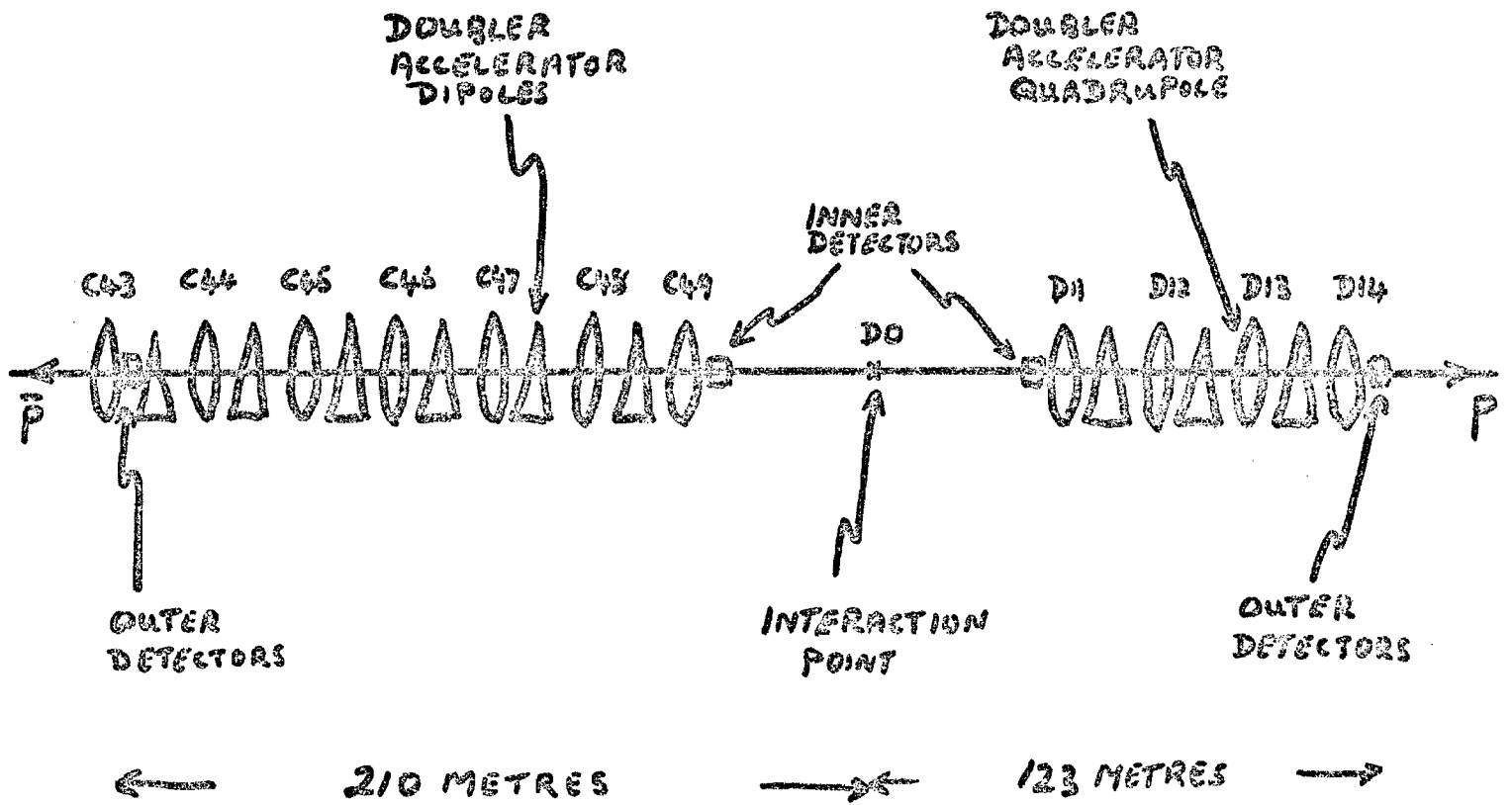


FIG. 7.

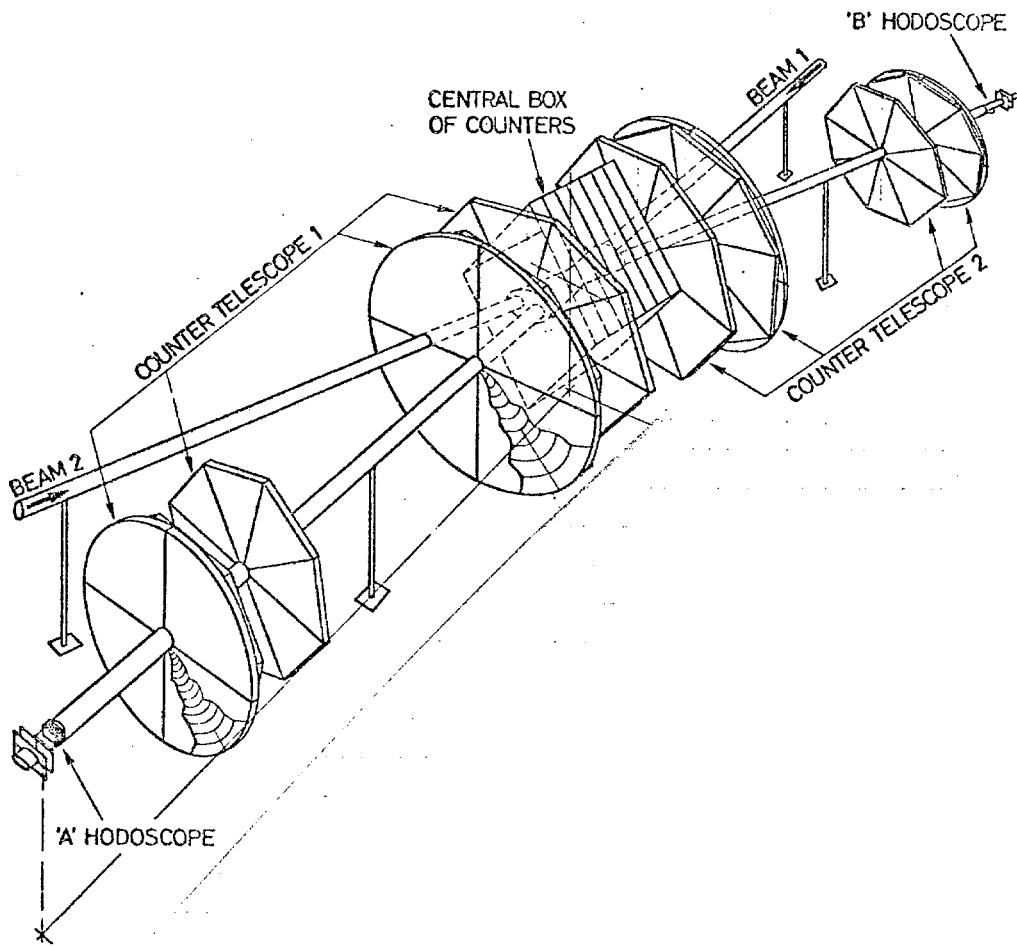


FIG. 8.

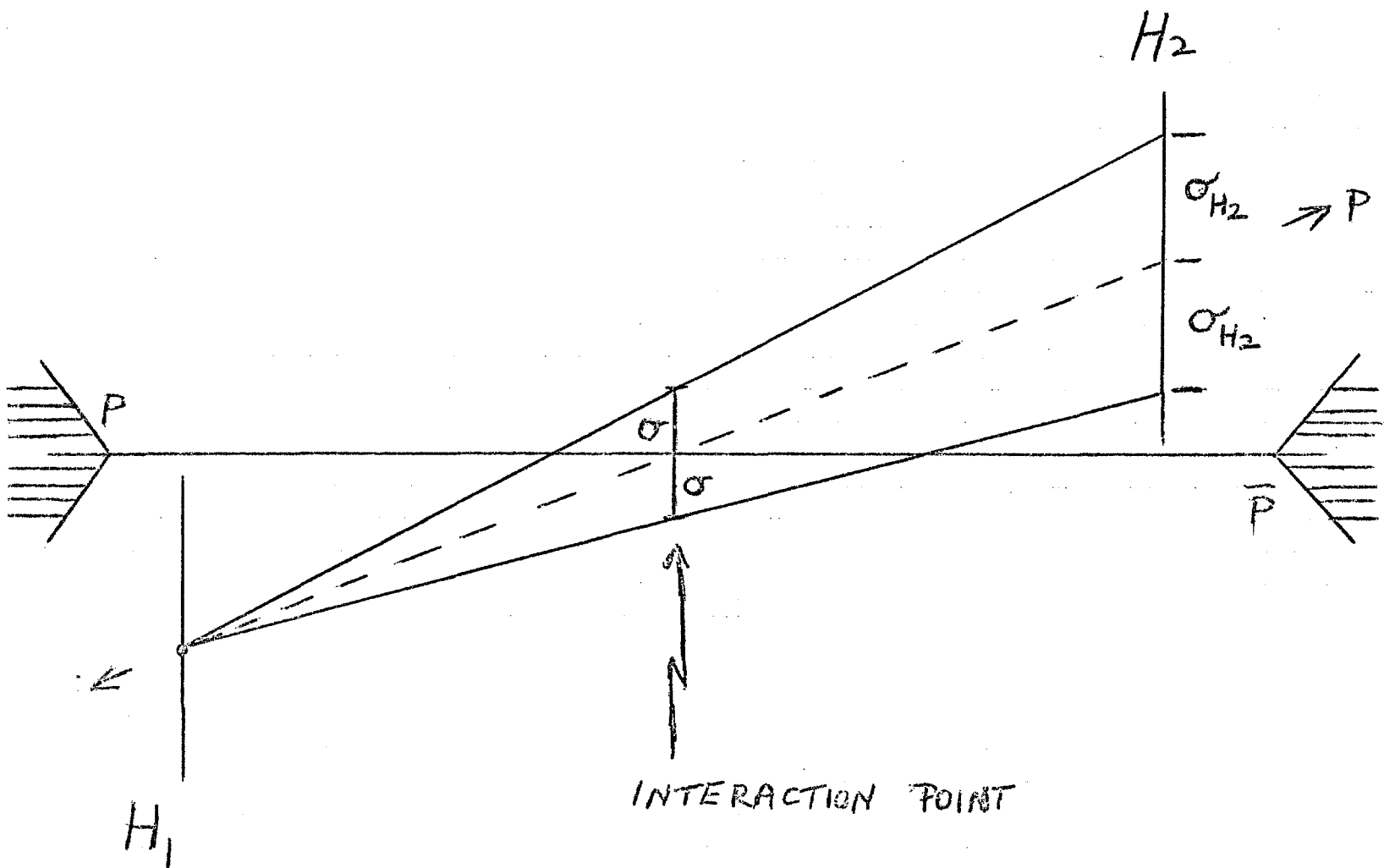


FIG. 9.